Antenna structure and excitation dynamics in photosystem I
II. Studies with mutants of *Chlamydomonas reinhardtii* lacking photosystem II

T. G. Owens,* S. P. Webb,‡ L. Mets,* R. S. Alberte,* and G. R. Fleming‡
*Department of Molecular Genetics and Cell Biology and ‡Department of Chemistry, The University of Chicago, Chicago, Illinois 60637

ABSTRACT Using time-resolved single photon counting, fluorescence decay in photosystem I (PS I) was analyzed in mutant strains of *Chlamydomonas reinhardtii* that lack photosystem II. Two strains are compared: one with a wild-type PS I core antenna (120 chlorophyll *a*/P700) and a second showing an apparent reduction in core antenna size (60 chlorophyll *a*/P700). These data were calculated from the lifetimes of core antenna excited states (75 and 45 ps, respectively) and from pigment stoichiometries. Fluorescence decay in wild type PS I is composed of two components: a fast 75-ps decay that represents the photochemically limited lifetime of excited states in the core antenna, and a minor (<10%) 300–800 ps component that has spectral characteristics of both peripheral and core antenna pigments. Temporal and spectral properties of the fast PS I decay indicate that (*a*) excitations are nearly equilibrated among the range of spectral forms present in the PS I core antenna, (*b*) an average excitation visits a representative distribution of core antenna spectral forms on all pigment-binding subunits regardless of the origin of the excitation, (*c*) reduction in core antenna size does not alter the range of antenna spectral forms present, and (*d*) transfer from peripheral antennae to the PS I core complex is rapid (<5 ps).

INTRODUCTION

The light-harvesting antennae of photosynthetic systems consist of highly ordered, protein-bound pigments. The spectral properties of these pigments are modified by interactions with their local environment, producing a range of antenna absorptions. A full understanding of the dynamics of excited-state energy transfer and photochemical trapping reactions within the antennae will require a characterization of the role of both spectral and spatial structure in these processes. In green algae and higher plant chloroplasts, this characterization is complicated by the presence of distinct antenna complexes with strongly overlapping spectral properties. Each spectral form of the antenna pigments can potentially make a unique contribution to parallel and sequential reactions of excited-state energy transfer and trapping. Although the transfer of a mobile excited state (excitation) between individual pairs of antenna pigments cannot be resolved in these complex systems, the spectral and kinetic properties of excitations averaged over functional aggregates of antenna pigments can, in principle, be measured. These kinetic and spectral properties provide, in turn, insight into structure/function relationships in the light-harvesting systems.

The application of time-resolved fluorescence spectroscopy using tunable dye laser pulsed excitation and single photon counting detection provides access to both spectral and kinetic information describing excitation decay (1). The high dynamic range of photon counting permits the resolution of complex multiexponential decays with time resolution of better than 10 ps (2, 3). The fluorescence decay of green algal cells or higher plant chloroplasts is characterized by at least four or five components (4) with lifetimes between 50 and 2,500 ps. The amplitudes and rate constants for each of these decay components are thought to be related to the relative absorption cross-section and to the kinetics of excitation transfer, trapping, and nonradiative decay (1). The time-resolved fluorescence excitation and emission spectra of the individual decay components provides information on the absorption and fluorescence properties of pigments contributing to that decay. The assignment of these decays to functional antenna aggregates has been a major focus of recent research in this area.

Because of the complexity and spectral overlap of these decay components in vivo, investigators have used a variety of techniques to alter or simplify samples for fluorescence decay analysis, thereby facilitating the assignment of the major fluorescence decay components. These include biochemical fractionation of the photosynthetic apparatus (5–10), chemical treatment of intact or fractionated samples (11–12), and genetic manipulation of the pigment-protein composition of thylakoid membranes (13–15). The results of these and other studies

T. G. Owens's present address is Section of Plant Biology, Cornell University, Ithaca, NY 14853-5908.

Address reprint requests to G. R. Fleming, Department of Chemistry, 5735 S. Ellis Ave., University of Chicago, Chicago, IL 60637.

0006-3495/89/07/95/12 $2.00

have led to the following general assignments. Two major decay components with 1/e lifetimes (τ) or ~0.3 and 0.6 ns are associated with the variable fluorescence yield of PS II. A minor component (τ = 2.5 ns) is assigned to uncoupled antenna complexes. Excitations in PS I–associated chlorophylls decay rapidly (τ = 75–95 ps) and exhibit a characteristic red shift of their spectral properties.

A detailed in vivo investigation of excitations localized in PS I is difficult due to their short lifetime and to the dominance of the PS II decay components. In previous investigations, we have examined the spectral and kinetic properties of PS I fluorescence decay in detergent-isolated preparations (2, 8, 9). Using both theoretical and experimental analyses, these studies have defined the general relationships between antenna structure and the dynamics of excitation transfer and trapping reactions in PS I. Our studies have distinguished between core and peripheral antenna pigments, where the core antenna consists of several spectral forms of chl *a* (120 chl *a*/P700) bound in the same protein complex that binds P700 (16, 17). In green algae and higher plants, the peripheral antenna complexes fall into two classes of light-harvesting chl *a*/*b*-binding complexes associated with either PS II (LHC II) or PS I (LHC I).

The present investigation describes the analysis of PS I fluorescence decay in several mutant strains of the green alga *Chlamydomonas reinhardtii*. These strains lack the PS II reaction center/core antenna complex and the decay components associated with PS II fluorescence. Fluorescence decay data confirm the presence of a second PS I decay component that has spectral characteristics of both the peripheral and core antennae. Simultaneous alterations in the content of LHC I and LHC II have both direct and indirect effects on excitation dynamics in the PS I core antenna. In one mutant, a 90% reduction in peripheral antenna complexes is associated with an apparent 50% reduction in the PS I core antenna size. Using a model of the pigment-protein stoichiometry of the PS I core antenna, the mutant fluorescence decay data provide information on the internal structure and excitation dynamics in the wild type PS I reaction center/core antenna complex.

MATERIALS AND METHODS

Culture conditions

Chlamydomonas reinhardtii strains 137c (wild type), 4D1c, A4d, B1, and other PS II-minus strains were grown mixotrophically in batch cultures on Tris-acetate-phosphate medium (18) at 22°C. Mutant B1 and related PS II-minus strains were selected by the metronidazole method (19) after treatment with 5-fluorodeoxyuridine. Strain B1 contains a deletion in the chloroplast *psb*A genes encoding the 32-kD herbicide-binding protein (Mets, L., unpublished data). Strain A4d was constructed by crossing B1 with 4D1c, a strain carrying the DS-521 mutation causing a deficiency in the chl *a*/*b*-binding proteins (Galloway and L. Mets, unpublished data). Cultures were grown under a continuous illumination of 100 μE $m^{-2}s^{-1}$ (wild type) or $\leq$1 μE $m^{-2}s^{-1}$ (mutant strains). Cells for time-resolved analyses were harvested by centrifugation and diluted in fresh medium to an absorbance of 0.1–0.2 at 675 nm.

Thylakoid isolation and polyacrylamide gel electrophoresis (PAGE)

Thylakoid membranes were isolated according to the procedure of Chua and Bennoun (20). Mutant strains accumulated large amounts of starch that were removed by exhaustive washing with 5 mM Tris HCl, 10 mM EDTA (pH 8.0) before the sucrose gradient step. Chlorophyll-protein complexes were separated on nondenaturing lithium dodecyl sulfate–PAGE at 4°C as described by Delepelaire and Chua (21); the pigment-protein nomenclature suggested by Thornber (22) was used. The distribution of chls *a* + *b* was measured by scanning gel slices at 662 nm (23) in a modified Cary-14 spectrophotometer (On-Line Instrument Systems, Inc., Jefferson, GA). Polypeptide composition of the thylakoid membranes was determined by using denaturing sodium dodecyl sulfate–PAGE (4°C) on a linear 7.5–15% acrylamide gradient (20). Thylakoid membrane polypeptides were numbered according to the scheme of Delepelaire and Chua (21). Isolation and quantitation of mutant LHC I content was accomplished using the procedures of Herrin et al. (24).

Pigment determination

Chlorophylls *a* and *b* were measured spectrophotometrically in 90% acetone extracts using the equations of Jeffrey and Humphrey (25). P700 was measured in thylakoid membranes solubilized in 1% Triton X-100 (Triton/chl = 60, wt/wt) by light-induced absorbance changes (26).

Spectroscopy

Room temperature fluorescence emission spectra (corrected for excitation intensity and detector sensitivity) were recorded using an optical multichannel analyzer (EGG-PAR OMA-III). Absorption spectra of whole cell suspensions were measured in a modified Cary-14 spectrophotometer with a laboratory-constructed integrating sphere.

Fluorescence decay kinetics were measured using time-resolved single photon counting as previously described (9, 14). Excitation was provided by a synchronously pumped, DCM dye laser (630–710 nm) that was cavity dumped at 75 kHz or 3.8 MHz (pulses 8–10 ps FWHM). Maximum excitation intensities were kept below 8×10^{10} photons cm^{-2} $pulse^{-1}$ for all samples. Samples were held in a temperature-regulated cuvette and gently stirred throughout the analyses. Fluorescence was collected at 90° to the excitation through a 700-μm slit and selected by a monochromator (bandwidth, 4 nm). Deconvolution of the instrument response function (60–70 ps, FWHM) from the measured fluorescence decay provided a time resolution of <10 ps. The quality of fit was assessed from the distribution of normalized residuals and the value of the reduced χ^2 parameter (<1.15 for "good" fits). Standard deviations on the mean lifetime of replicate samples varied from ±4 ps (τ = 20–80 ps) to ±33 ps (τ = 300–800 ps) and ±90 ps (τ = 1.5–2.5 ns). The temporal response of the system was calibrated by placing etalons in the excitation beam; performance of the system was frequently checked by measuring the single exponential decay of oxazine 725 in methanol (τ = 765 ± 10 ps at 21°C).

Time-resolved fluorescence excitation and emission spectra for each

decay component were calculated using the general treatment of Holzwarth and co-workers (1, 27) as described in Eq. 1

$$T_i(\lambda_{exc}, \lambda_{em}) = C \cdot A_i(\lambda_{exc}, \lambda_{em}) \cdot 1/N(I, \lambda_{exc}, \lambda_{em}). \quad (1)$$

Here, T_i is the relative time-resolved excitation or emission of decay component i at excitation and emission wavelengths λ_{exc} and λ_{em}, respectively, A_i is the preexponential amplitude of component i ($\Sigma A_i = 1$), N is the amount of time required to accumulate 10^4 counts in the peak decay channel at constant excitation intensity (I), and C is a constant. The steady-state emission of each decay component (S_i) was calculated from

$$S_i(\lambda_{exc}, \lambda_{em}) = C \cdot A_i(\lambda_{exc}, \lambda_{em}) \cdot \tau_i(\lambda_{exc}, \lambda_{em}) \cdot 1/N(I, \lambda_{exc}, \lambda_{em}), \quad (2)$$

where τ_i is the 1/e lifetime of decay component i. These calculations make no assumptions about the shape of the steady-state spectra. Spectra were corrected for detector sensitivity in all wavelength-dependent measurements.

RESULTS

Mutant characterization

The distribution of pigments in thylakoid membranes and isolated pigment-protein complexes from *C. reinhardtii* wild type strain 137c and mutant strains B1 and A4d is shown in Table 1. The deletion in the chloroplast *psb*A gene in strains B1 and A4d results in a complete loss of PS II activity: CO_2-dependent O_2 evolution and room temperature variable fluorescence are undetectable in both strains (Mets, L., unpublished results). Both strains also lack the two PS II core antenna complexes (CC II) associated with the PS II reaction center. In addition to the *psb*A deletion, strain A4d also contains the DS-521 nuclear mutation that causes a 90% reduction LHC II content and in total chl *b*/P700 (Table 1). Although at present there is no method of quantifying LHC I content in most strains of *C. reinhardtii*, we used the method of Herrin et al. (24) to prepare particles enriched in LHC I and CC I. These particles retain the low (20°C) fluorescence yield and long wavelength 77°K emission characteristic of LHC I/CC I aggregates (28). After mild dissociation of the particles and separation on nondenaturing gels, the ratio of total chl in the CC I and LHC I bands was found to be ~40% higher in strain A4d compared with strain B1 and wild-type (Table 1). *C. reinhardtii* strain 4D1c, which contains the DS-521 mutation but retains normal PS I and PS II activities, shows a similar change in pigment ratios and loss of LHC II complexes.

Analysis of thylakoid membrane polypeptides by denaturing SDS-PAGE (data not shown) demonstrates that neither B1 nor A4d accumulate the pigment-binding polypeptides of the PS II core antenna complex (mol wt = 47, 43 kD; polypeptides 5 and 6). In strains carrying the DS-521 mutation, there is a large reduction in three LHC II polypeptides (mol wt = 30.5, 25, and 24 kD; polypeptides 11, 16, and 17.1). The DS-521 mutation also alters the polypeptide composition of LHC I: polypeptide 15 (26 kD) is reduced whereas polypeptides 14 and 22 (27 and 20 kD) are present in excess of wild type. Polypeptide 18 (23 kD) is absent in strains carrying the DS-521 mutation. This protein has been assigned to LHC I (29) but could not be detected in wild type LHC I preparations (24). The molecular nature of the DS-521 mutation is unclear but it does not affect structural genes (chloroplast or nuclear) of the PS I core complex (Mets, L., unpublished data). Detailed biochemical analysis of these strains will be published elsewhere.

The steady-state absorption and fluorescence emission (20°C) spectra of wild type and mutant strains B1 and A4d are shown in Fig. 1. The absorption spectra reflect the variations in peripheral antenna content in the chl *b* absorption at 652 nm and minor shifts of the absorption maxima. The fluorescence emission spectra show the greatest variation in the long wavelength (685–740 nm) regions, resulting from increased contributions of PS I emission in the mutant strains (28, 30).

Time-resolved fluorescence analysis

The room temperature fluorescence decay (excitation at 670 nm, emission at 690 nm) of intact cell suspensions of

TABLE 1 Distribution of pigments, pigment-protein complexes, and photosystem activities in *C. reinhardtii* wild type strain 137c and mutant strains A4d and B1

	Photosystem activity		Whole cell ratios		Isolated pigment-proteins % total chlorophyll *a* + *b* on gel				Isolated LHC I/CC I aggregate % total chlorophyll *a* + *b*		
Strain	PS I	PS II	chl *a* + *b*/P700	chl *a*/*b*	CC I	LHC II	CC II	FP	CC I	LHC I	CC I/LHC I
137c	+	+	478 ± 48	2.64 ± .58	10	65	11	14	82	18	4.6
B1	+	–	366 ± 61	2.51 ± .39	11	73	0	16	84	16	5.2
A4d	+	–	117 ± 27	8.55 ± 1.8	80	8	0	12	89	11	8.1

PS I activity was measured as light-induced photobleaching at 697 nm, PS II activity as light-dependent oxygen evolution. Nomenclature for pigment protein complexes is according to Thornber (22): CC I and CC II, core antenna complexes of PS I and PS II; LHC II, peripheral light-harvesting complex of PS II; FP, free pigment. CC I/LHC I aggregates were isolated according to Herrin et al. (24).

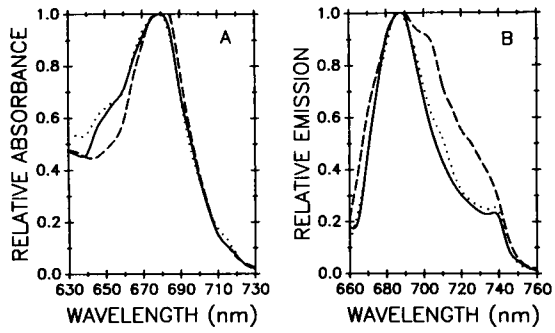

FIGURE 1 Room temperature (21°C), steady-state absorption, and fluorescence emission spectra for whole cell suspensions (corrected for scattering) of *C. reinhardtii* strains 137c (*solid line*), B1 (*dotted line*) and A4d (*dashed line*). (*A*) Absorption spectra; (*B*) fluorescence emission spectra.

C. reinhardtii strains A4d and B1 are accurately described ($\chi^2 < 1.15$) by three exponential components with lifetimes in the range of 40–90 ps, 300–800 ps, and 1.2–2.2 ns (Table 2). Addition of a fourth decay component led to a splitting of the long lifetime decay into two new components but did not statistically improve the fit. We did not observe rise components (negative preexponential amplitudes) of any lifetime in the decays even though such terms were routinely included in the range of initial estimates used for each regression analyses.

The three fluorescence decay components in strains A4d and B1 differ in both their relative amplitudes and lifetimes. The fast decay component in A4d has a lifetime of 43 ± 5 ps, whereas the same component in B1 has a lifetime of 76 ± 7 ps. Time-resolved analysis of seven other independently derived PS II-minus strains of *C. reinhardtii*, all with deletions in the *psb*A gene, gave an average lifetime of the fast decay component of 74 ± 6 ps. Lifetimes of 75–95 ps have been reported for PS I in several wild type strains of green algae and higher plant chloroplasts (for reviews see references 1, 31). Similarly, lifetimes of 10–40 ps have been reported for detergent-isolated PS I preparations (2, 5, 9). In all previous cases, the decays were attributed to the lifetime of excitations in the PS I core antenna. The differences in the lifetime of the fast decay component between A4d and other PS II-minus strains has been consistently observed for more than three years since the mutants were generated. We conclude that the differences are real and not due to artifacts of culture conditions or experimental methods.

TABLE 2 Fluorescence decay kinetics of *C. reinhardtii* strains A4d, B1, and seven independent PS II-minus mutants (including strain B1) measured at 652 nm excitation and 695 nm emission

Strain	A_1	τ_1	A_2	τ_2	A_3	τ_3
A4d	0.87	43 ± 5	0.09	345 ± 105	0.04	1350 ± 165
B1	0.43	76 ± 7	0.31	685 ± 155	0.26	1810 ± 215
All PS II⁻	0.52	74 ± 6	0.28	585 ± 130	0.20	1620 ± 300

Cells were obtained from midexponential phase cultures only. A_i and τ_i are the amplitudes and 1/e lifetimes of the three decay components in each sample. The decay parameters for A4d and B1 were averaged for 12 independent cultures over a period of two years. The PS II⁻ data is the average of seven independent PS II-minus strains carrying a deletion in the *psb*A gene: B1, 11-4d, D7, A8-36c, F8, A7, and LM18.

The lifetimes of the intermediate and slow decay components were also different in the two strains, but the differences were less significant. Fluorescence decay components with lifetimes in the range of 250–750 ps have been reported in membrane fractions enriched in PS I (9, 10, 27) and in algal mutants lacking PS II (8, 14, 15). Decay components with lifetimes in the range of 750–2,400 ps have been found in monomeric and oligomeric forms of LHC II in vitro (4, 6) and in *C. reinhardtii* strain C2, which lacks both the PS I and PS II reaction center/core antenna complexes (14, 32). The amplitudes of the three decay components also vary between strains A4d and B1. In strain A4d, the total decay is dominated (85–95%) by the 45 ps component; in B1 and the other PS II-minus strains, the fast decay (75 ps) contributes a maximum of ~50% to the decay (Table 2).

Spectral analysis of the decay components

The time-resolved fluorescence emission spectra (652 nm excitation) of the three decay components in strains A4d and B1 are presented in Figs. 2 and 3, respectively. In both strains, the predicted steady-state emission spectra (calculated using Eq. 2 and summing over all decay components) closely resemble the shape of the actual steady-state spectra (Fig. 2*C* and 3*C*). This establishes the validity of the time-resolved spectra. The contributions of the fast, intermediate, and slow decay components to total steady-state fluorescence (665–750 nm) are calculated to be 22, 28, and 50% in strain A4d and 6, 30, and 64% in strain B1, respectively. For the time-resolved spectra, the shape of the total spectrum (summed overall decay components) is completely determined by the $1/N$ term in Eq. 2. The contributions of individual decay components to the total time-resolved spectra are determined by the amplitudes A_i.

The normalized emission spectra of the fast (40–80 ps) decay components are very similar in strains A4d and B1, showing broad maxima between 680 and 700 nm (Figs. 2 *B* and 3 *B*). These spectra are similar to the emission spectrum of the 20–30–ps decay component in isolated PS I reaction center/core antenna complexes (9) with two important distinctions: (*a*) the maxima of the mutant in vivo spectra are broader and shifted to the red by 5–7 nm,

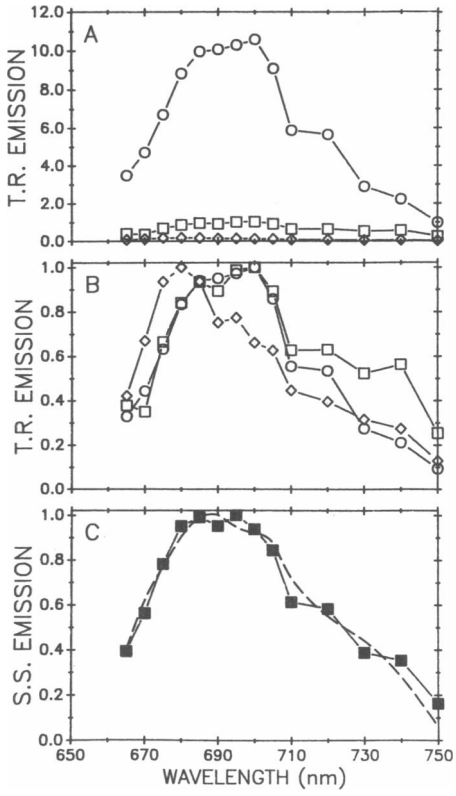

FIGURE 2 Time-resolved fluorescence emission spectra for whole cell suspensions of *C. reinhardtii* strain A4d (21°C, 652 nm excitation). (*Open circles*) Emission spectrum of 45 ps decay component; (*open squares*) spectrum of 350 ps decay; (*open diamonds*) spectrum of 1,350 ps decay; (*dashed line*) steady-state fluorescence emission spectrum; (*solid squares*) total time-resolved fluorescence emission. (*A*) Relative emission spectra of the three kinetic components; (*B*) emission spectra of the three decay components normalized at their respective maxima; (*C*) comparison of the total time-resolved and steady-state emission spectra.

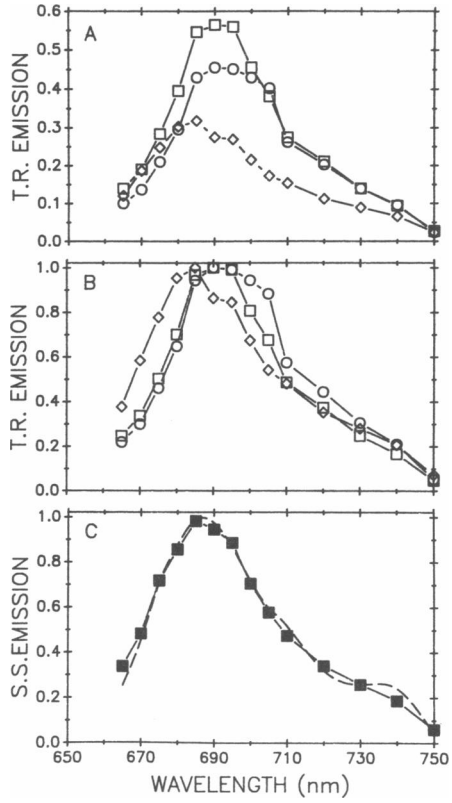

FIGURE 3 Time-resolved fluorescence emission spectra for whole cell suspensions of *C. reinhardtii* strain B1 (21°C, 652 nm excitation). (*Open circles*) Emission spectrum of 75 ps decay component; (*open squares*) spectrum of 800 ps decay; (*open diamonds*) spectrum of 1,800 ps decay; (*dashed line*) steady-state fluorescence emission spectrum; (*solid squares*) total time-resolved fluorescence emission. (*A*) relative emission spectra of the three kinetic components; (*B*) emission spectra of the three decay components normalized at their respective maxima; (*C*) comparison of the total time-resolved and steady-state emission spectra.

and (*b*) emission in the range of 700–740 nm is significantly greater in the mutants. The emission spectra of the 1.2–1.8–ns decay in A4d and B1 show a maximum near 680 nm characteristic of isolated LHC II complexes (6). The spectra are also very similar to the steady-state emission of the double mutant C2 that lacks both PS I and PS II core complexes (32).

In contrast to the similarities of the emission spectra of the fast and slow decay components, emission spectra of the 300–700 ps decay components in strains A4d and B1 differ significantly (Figs. 2*B* and 3*B*). In strain A4d, the intermediate decay exhibits a broad emission maximum between 680 and 700 nm, similar to the fast decay emission in both mutants and to the intermediate decay in detergent-isolated PS I preparations containing chl *b* (9). The A4d intermediate decay also shows enhanced emission at 720 to 740 nm. In contrast, the intermediate decay emission in B1 is centered at 690 nm with about one-half the bandwidth of A4d and has reduced emission at 720–750 nm.

The time-resolved fluorescence excitation spectra (720 nm emission) for the three decay components in A4d and B1 are shown in Figs. 4 and 5, respectively. Integration of the area under the individual decay components indicates that the fast, intermediate, and slow decay components contribute 88, 9, and 3% to the total time-resolved absorption cross-section in A4d and 58, 27 and 15% in B1. The normalized excitation curves for the intermediate and slow components of A4d and B1 are very similar, with a maximum at 675 and a ratio of 650 to 675 nm cross-sections of 0.72. These curves are similar to the absorption spectrum of the PS I and PS II-minus mutant C2 (32) and are characteristic of chl *a*/*b*–containing antenna complexes. The normalized excitation spectra of

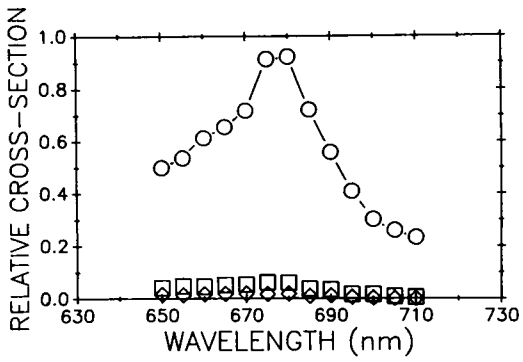

FIGURE 4 Time-resolved fluorescence excitation spectra of the three decay components in *C. reinhardtii* strain A4d (21°C, 720 nm emission). All spectra are expressed in units of relative absorption cross-section. Amplitudes of the time-resolved components show their relative contributions to the total fluorescence excitation. (*Open circles*) Excitation for 45 ps decay; (*open squares*) excitation for 350 ps decay; (*open diamonds*) excitation for 1,350 ps decay.

the fast decay components of A4d and B1 are similar with a broad maximum at 675–680 nm characteristic of the PS I core antenna pigments. However the fast decay components also show significant cross-sections at 652 and 675 nm associated with the absorption of the peripheral chl *a*/*b* antenna complexes. When normalized at the peak cross-section at 680 nm, the cross-section of strain B1 is 10–15% higher at 650–670 nm than that of A4d.

All three decay components show a weak dependence of fluorescence lifetime on emission wavelength, the dependence of each component being similar in both mutants. The lifetime of the fast decay component increases by 10–20% for emission wavelengths between 670 and 710 nm, then remain constants to 750 nm. This is in contrast to the fast decay lifetime in detergent-isolated PS I core complexes which is constant from 670 to 700 nm and then increase above 700 nm (9). The intermediate decay lifetimes increase by 20% between 670 and 750 nm in both A4d and B1, whereas lifetimes of the long decay decrease by 25–40% over the same wavelength range.

Variation in the lifetime of the PS I fast decay component with excitation wavelength is more pronounced in strains A4d and B1 than previously observed in detergent-isolated PS I preparations (9). Fig. 6 compares the excitation wavelength-dependence of the 45–75 ps decay component (720 nm emission) in A4d and B1 with those of detergent-isolated PS I preparations from barley and wild type *C. reinhardtii*. Regardless of the presence of peripheral antenna complexes, the detergent preparations show no significant variation with excitation wavelength. However, the fast decays of strains B1 and A4d show a 5–20 ps increase in lifetime below 670 nm, with a maximum lifetime near 650 nm. Between 670 and 700 nm, there is little lifetime variation among the samples.

The time-dependent evolution of the fluorescence emission spectrum (total emission from all decay components: $F[t,\lambda]$) following a δ-function excitation pulse can be calculated from the fluorescence decay kinetics at various emission wavelengths using the equation

$$F(t,\lambda) = [1/N(\lambda)] \cdot \Sigma A_i(\lambda) \exp[-t/\tau_i(\lambda)]. \quad (3)$$

Here, $A_i(\lambda)$ and $\tau_i(\lambda)$ are the kinetic constants of decay component i at emission wavelength λ and $N(\lambda)$ is a normalization factor that is equal to the relative amplitude of the steady-state fluorescence emission spectrum at wavelength λ. The data calculated for 652 nm excitation of A4d are shown in Fig. 7. The short wavelength

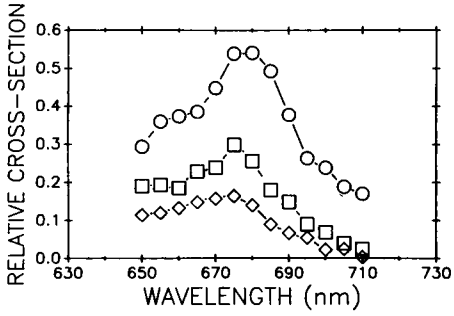

FIGURE 5 Time-resolved fluorescence excitation spectra of the three decay components in *C. reinhardtii* strain B1 (21°C, 720 nm emission). All spectra are expressed in units of relative absorption cross-section. Amplitudes of the time-resolved components show their relative contributions to the total fluorescence excitation. (*Open circles*) Excitation for 75 ps decay; (*open squares*) excitation for 800 ps decay; (*open diamonds*) excitation for 1,800 ps decay.

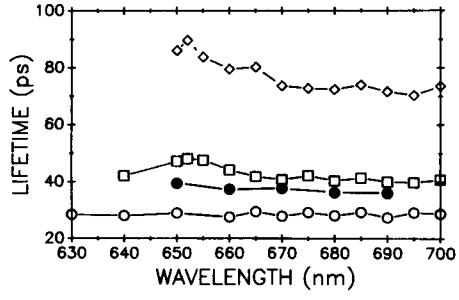

FIGURE 6 Dependence of the lifetime of the fast PS I decay component on excitation wavelength in detergent-isolated PS I preparations (10°C) and in *C. reinhardtii* strains A4d and B1 (21°C). Emission at 720 nm. (*Open circles*) Barley PS I preparation with 41 chl *a*/P700; (*solid circles*) *C. reinhardtii* (wild type) preparation containing 112 chl *a* + *b*/P700; (*open squares*) *C. reinhardtii* strain A4d; (*open diamonds*) *C. reinhardtii* strain B1.

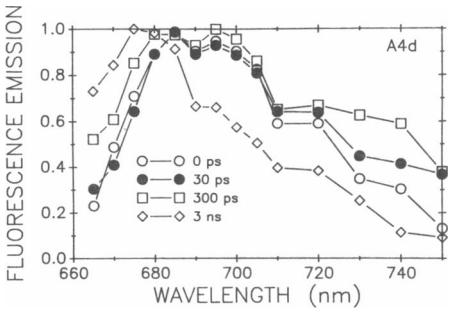

FIGURE 7 Time-dependent evolution of total fluorescence emission (summed over all decay components) in *C. reinhardtii* strain A4d. Spectra were calculated from the data in Fig. 3, see text for details. Excitation at 652 nm.

shoulder of the spectra shifts slightly (<5 nm) to longer wavelengths during the first 30 ps after the excitation pulse; subsequently, the spectrum shifts slowly to shorter wavelengths. Emission at 695–700 and 730–740 nm steadily increase for 300–500 ps after the pulse and then decrease for the remainder of the decay. Evolution of the emission spectrum in B1 is similar except the increase in emission at 720–740 nm is less pronounced and reaches a maximum at ~75 ps after the excitation pulse. These data are similar to those reported by Mimuro et al. (33) for detergent-free PS I preparations.

In a previous investigation, we conclude that excitations in the PS I core antenna are not rapidly concentrated within the longest wavelength absorbing spectral forms but are more nearly homogenized over all core antenna spectral forms during the lifetime of the excitation (9). This phenomenon was investigated directly in strain A4d by comparing the fluorescence decay at 695 nm for 680 nm excitation with replicate samples in which the excitation and emission wavelengths were reversed.

TABLE 3 Variations in the fluorescence decay kinetics in intact cell suspensions of *C. reinhardtii* strain A4d for excitation at 680 nm, emission at 695 nm versus excitation at 695 nm, emission at 680 nm

A_1	τ_1	A_2	τ_2	A_3	τ_3	N
680 nm excitation, 695 nm emission						
0.934	40.3	0.050	264	0.016	1660	1273 ± 41
695 nm excitation, 680 nm emission						
0.943	37.0	0.047	283	0.010	1970	8032 ± 181

Data are averages of three replicates at each excitation/emission wavelength. A_i and τ_i are the amplitudes and 1/e lifetimes of the three decay components. N is the time required to accumulate 10^4 counts in the peak fluorescence channel normalized to equal excitation intensities. Corrections to N were made for the transmission of blocking filters in the emission path.

The data, averaged for three replicates at each excitation wavelength, shows that the decay kinetics are nearly identical (Table 3), with only small changes in the amplitudes and lifetimes. The factor N represents the time (in seconds) required to accumulate 10^4 counts at a constant excitation intensity. Because the decays are similar, the value of N can be used to estimate the relative probabilities of fluorescence emission at each pair of excitation/emission wavelengths. When the values of N are corrected for the differences in sample absorption at 680 and 695 nm (A_{680}/A_{695} = 2.27) these data show that the probability of emission at 695 nm after 680 nm excitation is 2.8 times greater than emission at 680 nm from 695 nm excitation.

Effects of cations on decay kinetics

The concentration of divalent cations is known to affect the distribution of excitation energy between PS I and PS II in thylakoids of green algae and higher plants (34, 35). We investigated the effects of 0.1 and 5 mM Mg^{2+} on fluorescence decay kinetics in thylakoids isolated from strains A4d and B1 (Table 4). For 652 nm excitation, which is primarily absorbed by the peripheral chl *a*/*b* antenna complexes, there were no significant changes in the decay of strain A4d at the two cation concentrations. In strain B1, the lower Mg^{2+} treatment produced a significant increase in the amplitude of the intermediate decay component at the expense of the fast and slow components. In addition, the lifetime of the fast component increased from 73.4 ± 1.9 to 85.0 ± 0.9 ps upon reduction in Mg^{2+} concentration. Similar measurements for 680 nm excitation, absorbed primarily by the PS I core antenna, showed no effects of cation concentration on the fluorescence decay kinetics in strain A4d and only small differences in B1 (not shown).

TABLE 4 Effects of Mg^{2+} concentration on the fluorescence decay kinetics of thylakoid membranes isolated from *C. reinhardtii* strains A4d and B1

Strain	Mg^{2+}	A_1	τ_1	A_2	τ_2	A_3	τ_3
A4d	5.0	0.81	37.1	0.15	438	0.04	2259
A4d	0.1	0.81	36.8	0.15	450	0.04	2281
B1	5.0	0.35 ‡	73.4 §	0.35 ‡	588	0.30 *	1600
B1	0.1	0.28	85.0	0.48	606	0.24	1310

Excitation was at 652 nm, emission at 690 nm. Freshly prepared thylakoids (2 mg chl/ml) in 5 mM Hepes, 10 mM EDTA were diluted to a final chlorophyll concentration 20 g/ml, 0.3 M sucrose, 10 mM Hepes, and either 5.1 or 0.2 mM $MgCl_2$. Measurements were at 10°C. Significant differences at (*) 0.10, (‡) 0.025, and (§) 0.01 levels. Data are means of three replicates at each treatment.

DISCUSSION

In vivo studies of PS I-specific decay components are limited by our finite ability to resolve fast, low amplitude decays in the presence of the dominant emissions of PS II. In the present study, we have analyzed in vivo fluorescence decay in photosynthetic mutants of *C. reinhardtii* in which various PS II complexes have been deleted through genetic manipulations. Mutant strains A4d and B1 contain identical deletions in the chloroplast *psb*A gene leading to a loss of the CC II pigment-protein complexes and their constituent polypeptides, of PS II variable fluorescence and its associated decay components, and a total loss of PS II function. These pleiotropic effects associated with the loss of a functional *psb*A product have been observed previously (36). Strain B1 is highly fluorescent and exhibits a significant nanosecond decay component characteristic of uncoupled LHC II complexes. Strain A4d was constructed with the specific intent of reducing the high background fluorescence arising from uncoupled LHC II complexes in the absence of PS II. The amplitude of the slow decay component in strain A4d is comparable with that of wild type cells (3, 14, 27) indicating that the majority of peripheral complexes present (LHC I and LHC II) are coupled to the PS I core.

The short lifetimes and red-shifted fluorescence emission properties of the fast decay component in strains A4d and B1 suggest that this decay results from excitations in the PS I core antenna whose lifetime is limited by efficient photochemical quenching on P700 (2, 9). However, the lifetime of this decay component differs by about a factor of two between the two strains (45 ps for A4d, 75 ps for B1). In a previous study, we demonstrated a linear relationship between the lifetime of excitations in the PS I core antenna and the size of the core antenna (9). Based largely on PS I core lifetime measurements in strain A4d, and in disagreement with other biochemical studies (16, 17), we previously concluded (9) that the in vivo PS I core antenna size was 62 chl *a*/P700. We now consider this to be in error due to the discrepency in core antenna lifetimes between A4d and the other PS II-minus strains found in the present study. (Note that the only parameter of our lattice model calculations [9] that is sensitive to the core antenna size is the first passage time.)

Fig. 8 summarizes the relationship between lifetime of excitations in the PS I core antenna the total chl *a* + *b*/P700 in wild type and mutant strains of *C. reinhardtii* and in two detergent preparations. The data appear to segregate into three groups: detergent preparations with a maximum lifetime of 32 ps (core antenna size <45 chl *a*/P700 and total chl *a* + *b* <100/P700; *circles*), *C. reinhardtii* strains A4d and 4D1c (both carrying the DS-521 mutation, lifetimes of 40–45 ps; *squares*), and *C. reinhardtii* strain B1 and wild type (lifetimes of 75–85 ps; *diamonds*). Lifetimes of 75–85 ps were also observed in the seven independent *psb*A mutants (Table 2) as well as other species of green algae and chloroplasts of higher plants (1, 32).

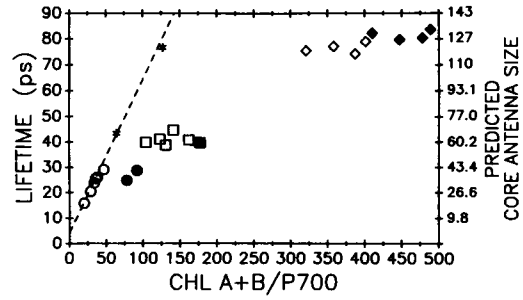

FIGURE 8 Summary of the lifetime of the fast PS I decay component as a function of the total antenna size (chl *a* + *b*) for detergent-isolated PS I preparations and three strains of *C. reinhardtii*. Dashed line shows the relationship between lifetime and PS I core antenna size for detergent-isolated preparations free of peripheral antenna pigments (2). Predicted PS I core antenna sizes (right *y*-axis) were determined for all samples from the relationship: antenna size = $1.67\tau - 7.01$ (2). (*Open circles*) Detergent-isolated PS I samples lacking chl *b*; (*solid circles*) detergent-isolated PS I samples containing chl *b*; (*open squares*) *C. reinhardtii* strain A4d; (*solid square*) strain LM3-4D1c (determined at F_m); (*open diamonds*) strain B1; (*solid diamonds*), wild-type strain 137c; (*asterisks*) relationship between the average core antenna size for strains A4d and B1 (65 and 125 chl *a*/P700, respectively) and average lifetime (τ_1) of excited states in each type of core antenna.

Also shown in Fig. 8 is the regression line of core antenna size against lifetime of the fast decay component from reference 2. As previously noted in detergent-isolated preparations (9), the relationship between lifetime and core antenna size does not extend to core plus peripheral antenna size. However, the average lifetimes suggest PS I core antenna sizes of ~120 chl *a*/P700 in wild type and B1, and 60 chl *a*/P700 in strains A4d and 4D1c (Fig. 8, *asterisks*). We note that although our PS I lifetime differs from that reported by Hodges and Moya (4, 15, 37), these authors also noted a decrease in PS I lifetime between PS II-minus and PS II-LHC II-minus mutants of *C. reinhardtii* (51 and 34 ps, respectively) (15).

A reduction in the PS I core antenna size of strain A4d is supported by two additional factors. First, a chl *a* + *b*/P700 ratio of <120 and chl *a*/*b* ratios between 6 and 8 are characteristic of midexponential phase A4d cultures and are inconsistent with a PS I core antenna size of 120 or even 100. Assuming a chl *a*/*b* ratio of 4 in LHC I (38, 39), these data suggest a core antenna size of ~60–65 chl *a*/P700. Second, detergent-isolated PS I core complexes have antenna sizes in the range of 100–120 or 40–50 chl *a*/P700, with the smaller complexes resulting

from more vigorous detergent treatments (16, 28, 40). The larger aggregates can be dissociated into smaller complexes (28, 40), one of which contains only core antenna pigments but maintains the in vivo 77°K emission properties of the core complex (41).

In detergent-isolated PS I preparations, the similarities of the time-resolved excitation and emission spectra of the fast decay component and the linear dependence of the lifetime of core excitations on the size of the core antenna suggest that excitations in the PS I core antenna were nearly equilibrated among the spectral forms of chl *a* present (2, 9). We have examined more directly the extent to which excitations are equilibrated among the in vivo core antenna spectral forms in strain A4d by measuring the relative core antenna fluorescence emission at 680 and 695 nm at two excitation wavelengths. With appropriate corrections for absorption and emission cross-sections, the probability for emission at 695 nm is 2.8 times greater than at 680 nm. This difference is reduced when considering that absorption by peripheral complexes at 680 nm contributes to 695 emission but that the converse is not true (see below). Assuming a Stokes shift of 5 nm and using the steady-state absorption to estimate the number of pigments functioning at each wavelength, the Boltzmann distribution predicts a 695–680–nm emission ratio of 2.2 for a fully equilibrated excitation. These data support the hypothesis that the average PS I core excitation is nearly equilibrated among a representative distribution of core antenna spectral forms during its lifetime. Measurements on strain B1 yielded qualitatively similar results although the increased contribution of uncoupled LHC II absorption at 680 nm complicates the analysis.

Although the PS I core antenna sizes in strains A4d and B1 appear to differ by about a factor of two, several factors indicate that the excitation dynamics are very similar in the two core antenna types. Each strain exhibits (*a*) similar core antenna absorption properties, (*b*) similar time-resolved emission spectra for the fast-decay component, (*c*) characteristics of excitations that are nearly equilibrated among the core antenna spectral forms, and (*d*) no variation in core antenna lifetime with excitation wavelengths between 680 and 700 nm. At present, our knowledge of the distribution of core pigments among the PS I core apoproteins is incomplete. At least two 60–70 kD proteins are required for binding of P700 and the initial PS I acceptors (42) and the wild-type antenna (120 chl *a*/P700) may require a total of two to six 60–70–kD proteins for pigment binding (16, 17, 43). Regardless of the exact distribution of core pigments and the mechanism causing the reduced core antenna size in strain A4d, the above data show that the pigment-binding subunits of the PS I core antenna do not function as separate units in energy transfer. During its migration to the reaction center, the average excitation must visit a representative distribution of pigments on each pigment-binding subunit regardless of the origin of the excitation. This description of excitation dynamics in PS I does not require a "funnel" type of antenna organization (44) for the core antenna and suggests that the spectral forms of the core antenna can be more randomly distributed in relation to the reaction center (9).

In contrast to previous in vitro preparations lacking peripheral antennae, strains A4d and B1 exhibit a pronounced excitation wavelength dependence of the fast decay component. Both strains exhibit an increase in lifetime in the region between 640 and 670 nm, where relative absorption by peripheral antenna complexes is maximal. In the main absorption of the core antenna (680–700 nm), the data show no excitation wavelength dependence. We suggest that the variations in the region of the peripheral antenna absorption may reflect the excitation transfer times from the point of origin in the peripheral antenna to the core complexes. These coupled peripheral antennae may include some LHC II in addition to LHC I. Due to the finite information content of photon counting curves, it is not possible to resolve the distinct rise and decay components (with equal lifetimes) that should arise from these transfers. Decays measured at wavelengths that excite both peripheral and core antennae may be artifactually prolonged due to unresolved lifetime contributions from transfers within the peripheral antenna as well as peripheral to core transfers. In strains A4d and B1, this results in an increase in core lifetime of ~5 and 20 ps, respectively. Because these strains have genetically altered thylakoid composition, we believe that the 5-ps increase represents an upper limit for the peripheral-to-core antenna transfer times in wild type PS I antennae. The observation that a linear relationship between lifetime and antenna size does not extend to core plus peripheral antenna sizes (Fig. 8) indicates that back transfer from the PS I core to peripheral antennae is limited.

The spectral and temporal properties of the 1.3–1.8–ns decay in strains B1 and A4d are very similar to those in the double mutant C2 (lacking both PS I and PS II) (14, 32) and isolated LHC II (4, 6). Together with the nanosecond lifetimes, these data support the assignment of this decay to peripheral (LHC I and/or LHC II) complexes that are unable to transfer excitations to core antennae aggregates. This assignment is confirmed by the time-dependent evolution of the total fluorescence emission spectrum, which shows the emission shifting the shorter wavelengths with increasing time after the excitation pulse. In strain B1, the lack of CC II as an organizational center for LHC II probably accounts for the large amplitude of the slow decay component. However, the difference between the amplitude of the nanosecond

decay component (A_3 = 0.26) and the fraction of chl *a* + *b* in LHC II (0.73, Table 1) suggests that much of the LHC II present in strain B1 is energetically coupled to the PS I core. Strain A4d lacks CC II, >90% of LHC II and may also contain alterations in the constituent polypeptides of LHC I. The low amplitude of the nanosecond decay component in strain A4d (A_3 = 0.04) is similar to wild type cells and suggests that most of the peripheral complexes, including any LHC II present, are functionally coupled to PS I.

The properties of the intermediate lifetime decay in strains A4d and B1 suggests that this component is complex in origin, with contributions from both peripheral and core antenna pigments. PS I–associated decays with lifetimes in the range of 300–800 ps have been reported by several authors (4, 5, 8, 14, 27). We noted previously that the occurrence of intermediate decay components was correlated with the presence of coupled peripheral antennae in detergent-isolated PS I complexes (9). Although the emission spectra of the intermediate decay show characteristics of excitations in the PS I core antenna, direct measurement of P700 oxidation rates (45) suggests that excitations contributing to this decay may not be used in photochemistry. Assuming that the properties of the intermediate decay are not due to membrane fractionation or genetic manipulation, we suggest that the wild type amplitude of this component is probably <10% of the total time-resolved PS I decay.

Divalent cations, in particular Mg^{2+}, are known to affect the rates of PS I electron transport (46), low-temperature fluorescence yield (34), and absorption cross-section of PS I (47). We observed that Mg^{2+} had no significant effect on the decay in either strain A4d or B1 when core antenna pigments were directly excited at 680 nm. This shows that Mg^{2+} has no direct effect on energy transfer or quenching processes in the PS I core antenna. For excitation at 652 nm, which is largely absorbed by chl *b* in the peripheral antenna, no Mg-dependent changes were observed in strain A4d but there were large changes in the decay of B1. Increasing Mg^{2+} from 0.1 to 5 mM decreased the relative amplitude of the intermediate decay (0.48 to 0.35) in relation to the amplitudes of the fast and slow components, and decreased the lifetime of the fast decay. Both the lifetime and amplitude effects in B1 are in the opposite sense to those predicted from previous measurements (46, 47) and may be related to nonphysiological aggregates of LHC II in the absence of PS II.

A lifetime of 75 ps for the fast decay component is consistent with a wild type core antenna size of 120 chl *a*/P700. The decrease in core antenna lifetime to 45 ps was only observed in those strains that carry the DS-521 mutation (A4d and 4D1c). Because the DS-521 mutation affects only the genes encoding the chl *a*/*b*-binding proteins (LHC II and LHC II) and not those of the PS I core complex, we suggest that the decreased core antenna lifetime (and apparent decrease in core antenna size) is the result of altered interactions between the peripheral antenna complexes and the PS I core. The nature of these interactions in strains carrying the DS-521 mutation is unknown, as is the role of these interactions in determining the structure of the core complex.

At the present time, the pigment-protein stoichiometry of the PS I reaction center/core antenna complex has not been resolved. Several studies have shown that two types of 60–70–kD proteins (products of the chloroplast *psa*A and *psa*B genes) (48) are sufficient to bind all 120 PS I core chlorophylls (16). Golbeck et al. (42) demonstrated that the minimum functional unit in vitro is a dimer of 60–70–kD polypeptides binding P700 and the initial PS I acceptors. The amino acid sequence of the *psa*A and *psa*B products suggests that each polypeptide may bind 30 or more core chlorophylls (49). Stoichiometries of two 60–70–kD polypeptides per P700 were originally reported by Bengis and Nelson and were recently supported by image analysis (43; Rogner, M., personal communication). Other studies have suggested four (17, 49, 50) or six (16) 60–70–kD units per P700. The apparent 50% reduction of the core antenna size in strain A4d and the ability to dissociate the "native" PS I complex (120 chl *a*/P700) into smaller subunits containing 40–60 chl *a*/P700 while maintaining photochemical activity (16, 28, 40) also supports complexes with more than two pigment-binding subunits. The simplest model for the PS I reaction center/core antenna complex that is consistent with these observations is one that contains four 60–70–kD polypeptides and 120 chl *a* per P700; two of the 60–70–kD subunits bind P700 and half of the core chl *a*, the other two subunits bind only the remaining 60 core chl *a*. We suggest that strain A4d and the smaller detergent preparations (<60 chl *a*/P700) lack the two subunits that bind only the core chlorophylls.

The authors wish to thank E. Castner and D. Eads for technical assistance with the laser systems, E. Wold for growing and maintaining the mutant strains, and B. Gulotty for his initial work on strain A4d.

This research was supported by grants from the National Science Foundation (DMB 8509590 and DCM 8409014). T. G. Owens was supported by a National Institutes of Health postdoctoral fellowship and a DuPont Young Faculty Award; S. P. Webb was supported by a gift from Amoco Corporation.

Received for publication 11 July 1988 and in final form 2 March 1989.

REFERENCES

1. Holzwarth, A. R. 1987. A model for the functional organization and energy distribution in the photosynthetic apparatus of higher

plants and green algae. *In* Progress in Photosynthesis Research. Vol. 1. J. Biggins, editor. Martinus Nijhoff, The Hague. 53–60.

2. Owens, T. G., S. P. Webb, L. Mets, R. S. Alberte, and G. R. Fleming. 1987. Antenna size dependence of fluorescence decay in the core antenna of photosystem I: estimates of charge separation and energy transfer rates. *Proc. Natl. Acad. Sci. USA.* 84:1532–1536.
3. Wendler, J., and A. R. Holzwarth. 1987. State transition in the green alga *Scenedesmus obliquus* probed by time-resolved chlorophyll fluorescence spectroscopy and global data analysis. *Biophys. J.* 52:717–728.
4. Hodges, M., and I. Moya. 1987. Time-resolved fluorescence studies on chloroplasts and green algae. Resolution of five kinetic components. *In* Progress in Photosynthesis Research. Vol. 1. J. Biggins, editor. Martinus Nijhoff, The Hague. 53–60.
5. Kamogawa, K., J. M. Morris, Y. Takagi, N. Nakashima, K. Yoshihara, and I. Ikegami. 1982. Picosecond fluorescence studies of P700-enriched particles for spinach chloroplasts. *Photochem. Photobiol.* 37:207–213.
6. Lotshaw, W. T., R. S. Alberte, and G. R. Fleming. 1982. Low-intensity subnanosecond fluorescence study of the light-harvestin chlorophyll a/b-protein. *Biochim. Biophys. Acta.* 682:75–85.
7. Holzwarth, A. R., W. Haehnel, J. Wendler, G. Suter, and R. Ratajczak. 1984. Picosecond fluorescence kinetics and energy transfer in antennae chlorophylls of green algae and membrane fractions of thylakoids. *In* Advances in Photosynthesis Research. Vol. 1. C. Sybesma, editor. Martinus Nijhoff, The Hague. 73–76.
8. Owens, T. G., S. P. Webb, D. D. Eads, R. S. Alberte, L. Mets, and G. R. Fleming. 1987. Time-resolved fluorescence decay in photosystem I: experimental estimates of charge separation and energy transfer rates. *In* Progress in Photosynthesis Research. Vol. 1. J. Biggins, editor. Martinus Nijhoff, The Hague. 83–86.
9. Owens, T. G., S. P. Webb, R. S. Alberte, L. Mets, and G. R. Fleming. 1988. Antenna structure and excitation dynamics in photosystem I. I. Studies of detergent-isolated photosystem I preparations using time-resolved fluorescence analysis. *Biophys. J.* 53:733–745.
10. Wittmershaus, B. P., D. S. Berns, and C. Huang. 1987. Picosecond time-resolved fluorescence from detergent-free photosystem particles. *Biophys. J.* 52:829–836.
11. Nairn, J. A., W. Haehnel, P. Reisberg, and K. Sauer. 1982. Picosecond fluorescence kinetics in spinach chloroplasts at room temperature. Effects of Mg^{2+}. *Biochim. Biophys. Acta.* 682:420–429.
12. Karukstis, K. K., and K. Sauer. 1985. The effects of cation-induced and pH-induced membrane stacking on chlorophyl fluorescence decay kinetics. *Biochim. Biophys. Acta.* 806:374–388.
13. Green, B. R., K. K. Karukstis, and K. Sauer. 1984. Fluorescence decay kinetics of mutants of corn deficient in photosystem I and photosystem II. *Biochim. Biophys. Acta.* 767:574–581.
14. Gulotty, R. J., L. Mets, R. S. Alberte, and G. R. Fleming. 1985. Picosecond fluorescence study of photosynthetic mutants of *Chlamydomonas reinhardii:* origin of the fluorescence decay kinetics of chloroplasts. *Photochem. Photobiol.* 41:487–496.
15. Hodges, M., and I. Moya. 1987. Time-resolved chlorophyll fluorescence studies on photosynthetic mutants of *Chlamydomonas reinhardtii:* origin of the kinetic decay components. *Photosynth. Res.* 13:125–141.
16. Vierling, E., and R. S. Alberte. 1983. P700 chlorophyll *a*-protein. Purification, characterization and antibody preparation. *Plant Physiol.* 72:625–633.
17. Lundell, D. J., A. N. Glazer, A. Melis, and R. Malkin. 1985. Characterization of a cyanobacterial photosystem I complex. *J. Biol. Chem.* 260:646–654.
18. Surzycki, S. 1971. Synchronously grown cultures of *Chlamydomonas reinhardii. Methods Enzymol.* 23:67–73.
19. Schmidt, G. W., K. S. Maltin, and N.-H. Chua. 1977. A rapid procedure for selective enrichment of photosynthetic electron transport mutants. *Proc. Natl. Acad. Sci. USA.* 74:610–614.
20. Chua, N.-H., and P. Bennoun. 1975. Thylakoid membrane proteins of *Chlamydomonas reinhardii:* wild-type and mutant strains deficient in photosystem II reaction centers. *Proc. Natl. Acad. Sci. USA.* 72:2175–2179.
21. Delepelaire, P., and N.-H. Chua. 1981. Lithium dodecyl sulfate/polyacrylamide gel electrophoresis of thylakoid membranes at 4C: characterization of two additional chlorophyll *a*-protein complexes. *Proc. Natl. Acad. Sci. USA.* 76:111–115.
22. Thornber, J. P. 1986. Biochemical organization and structure of pigment-proteins of photosynthetic organisms. *In* Photosynthesis III. Photosynthetic Membranes and Light-harvesting Systems. L. A. Staehelin and C. J. Arntzen, editors. Springer-Verlag, Berlin. 98–142.
23. Evans, J. R., and J. M. Anderson. 1987. Absolute absorption and relative fluorescence excitation spectra of the five major chlorophyll-protein complexes from spinach thylakoid membranes. *Biochim. Biophys. Acta.* 892:75–82.
24. Herrin, D. L., F. G. Plumley, M. Ikeuchi, A. S. Michaels and G. W. Schmidt. 1987. Chlorophyll antenna proteins of photosystem I: topology, synthesis, and regulation of the 20-kDa subunit of *Chlamydomonas* light-harvesting complex of photosystem I. *Arch. Biochem. Biophys.* 254:397–408.
25. Jeffrey, S. W., and G. F. Humphrey. 1975. New spectrophotometric equations for determining chlorophylls a, b, c_1 and c_2 in higher plants, algae and natural phytoplankton populations. *Biochem. Physiol. Pflanz. (BPP).* 167:191–194.
26. Shiozawa, J. A., R. S. Alberte, and J. P. Thornber. 1974. The P700-chlorophyll a-protein. Isolation and some characteristics of the complex in higher plants. *Arch. Biochem. Biophys.* 165:388–397.
27. Holzwarth, A. R., J. Wendler, and W. Haehnel. 1985. Time-resolved picosecond fluorescence of the antenna chlorophylls in *Chlorella vulgaris.* Resolution of the photosystem I fluorescence. *Biochim. Biophys. Acta.* 807:155–167.
28. Mullet, J. E., J. J. Burke, and C. J. Arntzen. 1980. Chlorophyll proteins of photosystem I. *Plant Physiol.* 65:814–822.
29. Wollman, F.-A., and P. Bennoun. 1982. A new chlorophyll-protein complex related to photosystem I in *Chlamydomonas reinhardii. Biochim. Biophys. Acta.* 680:352–360.
30. Kyle, D., N. Baker, and C. J. Arntzen. 1983. Spectral characteristics of photosystem I fluorescence at room temperature using thylakoid protein phosphorylation. *Photobiochem. Photobiophys.* 5:11–25.
31. Geacintov, N. E., and J. Breton. 1987. Energy transfer and fluorescence mechanisms in photosynthetic membranes. *CRC Crit. Rev. Plant Sci.* 5:1–44.
32. Eads, D. D., S. P. Webb, T. G. Owens, L. Mets, R. S. Alberte, and G. R. Fleming. 1987. Characterization of fluorescence decay in the chlorophyll a/b-protein. *In* Progress in Photosynthesis Research. Vol. 1. J. Biggins, editor. Martinus Nijhoff, The Hague. 135–138.
33. Mimuro, M., I. Yamazaki, N. Tamai, T. Yamazaki, and Y. Fugita. 1987. Analysis of excitation energy transfer in spinach chloro-

plasts at room temperature. Identification of the component bands by the time-resolved fluorescence spectrum and convolution of the decay kinetics. *In* Primary Processes in Photobiology. T. Kobayashi, editor. Springer-Verlag, Berlin. 23–32.

34. Murata, N. 1969. Control of excitation transfer in photosynthesis II. Magnesium ion-dependent distribution of excitation energy between two pigment systems in spinach chloroplasts. *Biochim. Biophys. Acta.* 189:171–181.
35. Fork, D. C., and K. Satoh. 1986. The control by state transitions of the distribution of excitation energy in photosynthesis. *Annu. Rev. Plant Physiol.* 37:335–261.
36. Bennoun, P., M. Spierre-Herz, J. Erickson, J. Girard-Bascou, Y. Pierres, M. Delosme, and J.-D. Rochaix. 1986. Characterization of photosystem II mutants of *Chlamydomonas reinhardii* lacking the psbA gene. *Plant Mol. Biol.* 6:151–160.
37. Hodges, M., and I. Moya. 1986. Time-resolved chlorophyll fluorescence studies of photosynthetic membranes: resolution and characterization of four kinetic components. *Biochim. Biophys. Acta.* 849:193–202.
38. Lam, E., W. Oritz, S. Mayfield, and R. Malkin. 1984. Isolation and characterization of a light-harvesting chlorophyll a/b-protein associated with photosystem I. *Plant Physiol.* 74:650–655.
39. Anderson, J. M. 1984. A chlorophyll a/b-protein of photosystem I. *Photobiochem. Photobiophys.* 8:221–228.
40. Malkin, R. 1986. A consideration of the organization of chloroplast photosystem I. *Photosynth. Res.* 10:197–200.
41. Sonoike, K., and S. Katoh. 1986. Isolation of an intrinsic antenna chlorophyll a-protein from the photosystem I reaction center of the thermophilic cyanobacterium *Synechococcus sp. Arch. Biochem. Biophys.* 244:254–260.
42. Golbeck, J. H., A. E. McDermott, W. K. Jones, and D. M. Kurtz. 1987. Evidence for the existence of [2Fe-2S] as well as [4Fe-4S] clusters among F_A, F_B, and F_x. Implication for the structure of the photosystem I reaction center. *Biochim. Biophys. Acta.* 891:94–98.
43. Boekema, E. J., J. P. Dekker, M. G. van Heel, M. Rogner, W. Saenger, I. Witt, and H. T. Witt. 1987. Evidence for a trimeric organization of the photosystem I complex from the thermophilic cyanobacterium *Synechococcus sp. FEBS (Fed. Eur. Biochem. Soc.) Lett.* 217:283–286.
44. Seely, G. R. 1973. Energy transfer in a model of the photosynthetic unit of green plants. *J. Theor. Biol.* 40:189–199.
45. Tristl, H.-W., W. Leibl, J. Deprez, A. Dobek, and J. Breton. 1988. Trapping and annihilation in the antenna system of photosystem I. *Biochim. Biophys. Acta.* 893:320–332.
46. Bose, S., J. E. Mullet, G. E. Hoch, and C. J. Arntzen. 1981. Effects of cations on photosystem I electron transport. *Photobiochem. Photobiophys.* 2:45–52.
47. Telfer, A., H. Bottin, J. Barber, and P. Mathis. 1984. The effects of magnesium and phosphorylation of light-harvesting chlorophyll a/b-protein on the yield of P700-photooxidation in pea chloroplasts. *Biochim. Biophys. Acta.* 764:324–330.
48. Fish, L. E., U. Kuck, and L. Bogorad. 1985. Two partially homologous adjacent light-inducible maize chloroplast genes encoding polypeptides of the P700 chlorophyll a-protein complex of photosystem I. *J. Biol. Chem.* 260:1413–1419.
49. Cantrell, A., and D. A. Bryant. 1987. Molecular cloning and nucleotide sequence of the pea psaA and psaB genes of the cyanobacterium *Synechococcus* PCC 7002. *Plant Mol. Biol.* 9:453–468.
50. Bruce, B. D., and R. Malkin. 1988. Subunit stoichiometry of a chloroplast photosystem 1 complex. *J. Biol. Chem.* 263:7302–7308.